

# Petrochemistry of Sediment and Organic Materials Sampled from Ossuaries and Two Nails from the Tomb of the Family of the High Priest Caiaphas, Jerusalem

Aryeh E. Shimron<sup>1</sup>, Yoetz Deutsch<sup>1</sup>, Werner H. Schoch<sup>2</sup>, Vitaly Gutkin<sup>3</sup>

<sup>1</sup>Geological Survey of Israel (Ret.), Jerusalem, Israel

<sup>2</sup>Labor Fur Quartere Holtzer, Langnau, Switzerland

<sup>3</sup>The Center for Nanoscience and Nanotechnology, The Hebrew University of Jerusalem, Jerusalem, Israel

Email: aeshimron@gmail.com

**How to cite this paper:** Shimron, A. E., Deutsch, Y., Schoch, W. H., & Gutkin, V. (2020). Petrochemistry of Sediment and Organic Materials Sampled from Ossuaries and Two Nails from the Tomb of the Family of the High Priest Caiaphas, Jerusalem. *Archaeological Discovery*, 8, 260-287. <https://doi.org/10.4236/ad.2020.83015>

**Received:** June 16, 2020

**Accepted:** July 10, 2020

**Published:** July 13, 2020

Copyright © 2020 by author(s) and Scientific Research Publishing Inc. This work is licensed under the Creative Commons Attribution International License (CC BY 4.0).

<http://creativecommons.org/licenses/by/4.0/>



Open Access

## Abstract

We have studied the petrochemistry of degraded bones and sediment from the interior of four ossuaries (burial boxes) discovered in what is (arguably) believed to be the 1<sup>st</sup> century CE family tomb of the high priest Caiaphas (herewith Cft) in Jerusalem. During the course of the 1990 excavation, among other artifacts (e.g., a coin found in a skull) two iron nails were discovered. One of the nails was inside an ossuary, the other on the floor of one of the nearby “kokhim” (burial niches) which contained Ossuaries 5 and 6. According to the Israel Antiquities Authority (IAA) everything in the burial cave can be accounted for today except the iron nails “*which have been misplaced*”, this without being properly recorded or photographed. Investigative journalist Simcha Jacobovici believes that he has located the nails in the artifacts collection of the Anthropology laboratory at Tel Aviv University. The IAA, however, has stated that the lost nails from the Cft have nothing to do with the nails found at the university and the latter nails must have a different provenance. Wherever lies the truth, the presence of two nails in the Cft is of profound interest because in the New Testament the high priest Caiaphas was responsible for passing Jesus to the Romans who then sent him to the cross. The possibility that the nails were used in a crucifixion on the one hand and can be connected to Caiaphas the high priest on the other is, to say the least, interesting and potentially monumental. Aware of the controversy but also of the importance of the two unprovenanced nails we have investigated the materials which have invaded the interiors of the Cft ossuaries and in a similar manner materials that have adhered to the two unprovenanced nails. Em-

ploying geochemical and petrochemical Scanning Electron Microscope (SEM-EDX), X-ray diffraction (XRD) and  $\delta^{18}\text{O}$  and  $\delta^{13}\text{C}$  isotope analyses we have found that the organic and inorganic materials flushed into the interior of the Cft but also those that have adhered to the two unprovenanced nails possess and display many identical, and what can also be termed unique chemical and physical characteristics. *Based on the collective evidence we conclude, with considerable confidence, that the unprovenanced nails are the lost nails excavated from the Caiaphas family tomb in 1990 and furthermore that these nails were used in a crucifixion.*

## Keywords

Jerusalem, Caiaphas Tomb Ossuaries, Crucifixion Nails, Accreted Cedar Wood, Tracheids, Microbial Infestation, Bone Degradation, Lepidocrocite, Goethite, Magnetite, Botryoids, Accretion Rims, Fungal Sporangium, Spores, Hyphae, Bone Microfabric, Yeast Cells, Trabeculae, Bacterial Biofilm, Hellenistic Period Aqueduct, SEM, XRD and  $\delta^{18}\text{O}$   $\delta^{13}\text{C}$  Isotopes

## 1. Introduction

*“There is no proof whatsoever that those nails came from the cave of Caiaphas. There is no proof that the nails are connected to any bones, or that there is any bone residue attached to the nails. There is no proof from textual data that Caiaphas had the nails from the crucifixion with him after the crucifixion took place and after Jesus was taken down from the cross.*

(Prof. Gaby Barkai, Telegraph, UK, 12 April, 2011).”

Such lofty declarations and academic disputes pertaining to the Caiaphas family tomb and two (arguably) crucifixion nails found therein have in major part been confined to the media and scholars in the fields of archaeology, anthropology and divinity. Besides the excavators few, if any, have examined or studied the ossuaries from the Cft (Caiaphas family tomb) and certainly not the nails above, was of adequate merit to inspire the scientific efforts below. Although the route following the present endeavours is rather lengthy we trust that what we here view as an original contribution not only to scientific thought of artifacts discovered in ancient ossuaries but also to Christianity at its very earliest, do these efforts justice.

What is referred to as the Caiaphas family tomb was discovered by construction workers in 1990 in the Jerusalem neighborhood of North Talpiyot, located about halfway between ancient Jerusalem and Bethlehem (**Figure 1**). The Cft is one of three tombs located within ~200 meters and less of the Lower (Hellenistic period, 1<sup>st</sup> - 2<sup>nd</sup> century BC) aqueduct with (arguably) all displaying some evidence of early Christianity (Tabor and Jacobovici, 2012; Shimron et al., 2020). The Cft was broken into by tomb robbers, probably during the Byzantine period. Except for Ossuaries 5 and 6 which were found in their kokhim with their lids

on, all ossuaries were moved from their rock shelves (Greenhut, 1992, 2004) at this time. Ossuaries 1, 2, 3, and 4 were found whole whereas six additional ossuaries were found shattered but were later reconstructed by the Israel Antiquities Authority (IAA). A total of 12 ossuaries were removed from the tomb during the archaeological excavation. The exterior walls of five ossuaries are inscribed, and six are decorated with floral motifs, Ossuary 6 magnificently so (Greenhut, 1992, **Figure 2(b)**). The name “Caiapha” is inscribed on the latter and also on Ossuary 3. A coin of Herod Agripa 1 from the year 42 - 43 CE was discovered in the scull inside Ossuary 8, besides precisely dating the tomb it also points to the pagan custom of placing a coin between the teeth of the deceased as payment to Charon, the ferryman in Greek mythology (Toynbee, 1971) thus pointing to the usage of this pagan custom in Jewish Jerusalem during this period (Hachlili & Killebrew, 1983; Tabor & Jacobovici, 2012). Most scholars agree with the excavators that the inscribed names refer to the family of the 1<sup>st</sup> century CE Jewish high priest Caiapha, transliterated “Caiaphas” in the New Testament.

Two iron nails were discovered during excavation of the tomb (Greenhut, 1992), one on the floor of the southern loculus (kokh IV) in which ossuaries 5 and 6 were contained, the other, according to the head excavator (Greenhut, 2004) inside Ossuary 1. Regarding the function of the nails, Rahmani (1961) suggested that nails found in tombs were used for fixing ossuary lids or for scratching the name of the deceased on an ossuary’s side. This interpretation remains prevalent and is thus far the only opinion expressed in academic circles. Consequently, the official IAA statement that the nails uncovered in the tomb during its excavation were misplaced or transferred to some unknown location did not cause any clamour.

About 20 years ago, Prof. I. Hershkovitz of the Sackler School of Medicine and Anthropology laboratory at Tel Aviv University received from the IAA two small boxes. One box was clearly marked as originating from the laboratory of the late Prof. Nicu Hass; the other box, which held two nails, was unmarked and the provenance of the nails that it contained was not specified. The two boxes were stored in the laboratory’s safe. A few years ago Prof. Israel Hershkovitz showed them to journalist Simcha Jacobovici who, based on his investigation of the Caiaphas family tomb finds, hypothesized that the two unprovenanced nails in the unmarked box were the missing nails from the Cft (Jacobovici, 2014). He further surmised that, given their morphology, these nails may have been used in a crucifixion and furthermore, in view of their archaeological context (tomb of the high priest Caiaphas) the crucifixion may have been that of Jesus of Nazareth. Thus far the only unambiguous physical evidence of nails used in a crucifixion is the 11.5 cm long Heel Bone nail from the crucifixion of Yehohanan Ben Hagoal discovered in a Jerusalem tomb in 1968. The gravity of these implications have led us to carry out the present in-depth scientific investigation of materials in the Caiaphas tomb ossuaries and also of the two unprovenanced nails from Prof. Hershkovitz’s laboratory. Such a geochemical-petrochemical study of

provenancing materials excavated from tomb ossuaries has, to the best of our knowledge, only one precedent—our recently published study on the ossuaries and materials from the nearby Talpiot—“Jesus family” tomb (Shimron et al., 2020, and Figure 1).

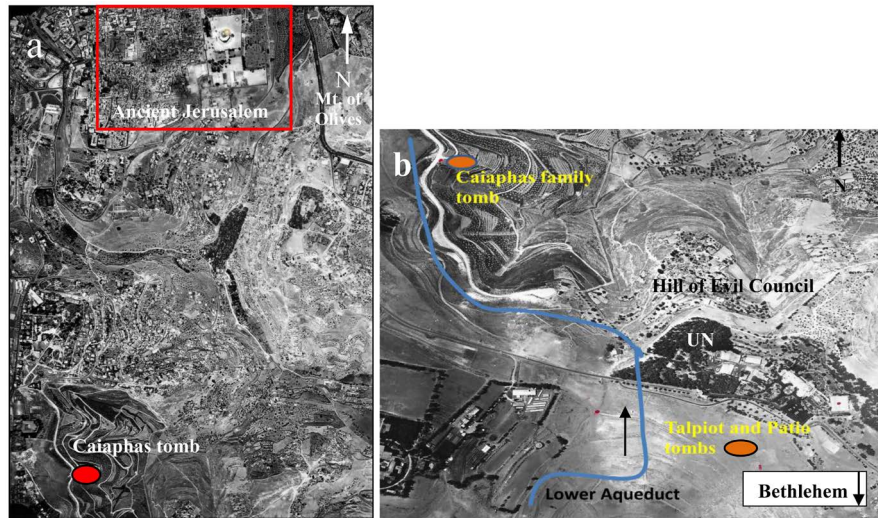


**Figure 1.** (a) 1970 aerial photographs showing the setting of the Caiaphas family tomb. (b) East Talpiot quarter and the biblical Hill of Evil Council (now the UN compound) neighborhood in SE Jerusalem. The Lower (Hellenistic period) aqueduct is in blue, the arrow points from the S to N direction of water flow. Photo base: Israel Mapping Center (1971).

## 2. Sampling and Analytical Procedures

Sampling of sediment flushed into the Caiaphas tomb ossuaries was carried out by technician Oded Reviv of the IAA. A few grams (about 1 - 2 teaspoonfuls) of loose sediment and/or fine rubble were collected from ossuaries 1, 3, 6 and 7 (a repaired ossuary) using a stainless steel spatula. Occasionally this was not feasible, in such case, sediment was scraped off from the ossuary bottom and/or ossuary walls (laminated wall crusts) with a stainless steel scalpel. Grain mounts for the scanning electron microscope (SEM) and polished and regular thin sections for study in transmitted light optical microscope were prepared from fine materials. The two unprovenanced nails were sampled in the laboratory of the Dept. of Anthropology, Tel Aviv University. This was carried out by the senior author (AES) using a specially prepared stainless steel holder on which a small diamond bit was mounted. As sampling small artifacts is a destructive process only a small amount (maximum 1/4 teaspoonful) of rusted iron and carbonate carapace could be scrapped off from the oxidized surface of each nail. These materials were studied under the petrographic and scanning electron microscope and analyzed by SEM-EDX, X-ray diffraction (XRD) and  $\delta^{18}\text{O}$  and  $\delta^{13}\text{C}$  isotopic analyses. Prior to the above studies, the nails were examined and photographed intact under low power SEM magnification.

X-ray diffraction analyses were done at the geochemical laboratory of the

Israel Geological Survey using a Philips XRD diffractometer with the following equipment: 1. High tension generator—PW1830 operated at tension of 40 KV and a current of 30 mA, 2. Philips MPD control—PW 3710, 3. Philips Goniometer—PW 3020, operating with a Cu long fine focus PW—2773/00 target, 4. Slit system: divergence slit—1°, 5. CuK $\beta$  radiation was eliminated with the aid of a Philips PW 1752/00 Monochromator. The <200 mesh ground samples were inserted in the diffractometer in a standard Philips rectangular aluminum sample holder.

Scanning Electron Microscope (SEM-EDX) analyses were carried out at the Hebrew University Nanolaboratory (The XPS Laboratory Unit for Nanocharacterization, The Harvey M. Krueger Center for Nanoscience and Nanotechnology in Jerusalem) by Dr. Vitaly Gutkin (supervisor of the unit) and AES—the senior author. The scanning electron microscopy images were obtained using an FEI Quanta 200 ESEM in low-vacuum mode without any preliminary treatment and with a chamber pressure of 0.38 Torr and acceleration voltages of 15 - 20 kV. Elemental analyses were carried using EDX (Energy Dispersive X-Ray spectroscopy). Energy Dispersive X-Ray Spectroscopy is a chemical microanalysis technique used in conjunction with SEM. The EDX technique detects X-rays emitted from the sample during bombardment by an electron beam to characterize the elemental composition of the analyzed volume. All photos used in this manuscript, unless denoted otherwise, are SEM micrographs.

Stable isotope  $\delta^{18}\text{O}$  and  $\delta^{13}\text{C}$  measurements were performed using a Gas Bench system attached to a Delta Plus mass spectrometer (Thermo). All  $\delta^{18}\text{O}$  and  $\delta^{13}\text{C}$  values were calibrated against the international standard NBS-19, and are reported in permil (‰) relative to the VPDB standard. Analytical reproducibility of duplicates is better than 0.1‰ both for  $\delta^{18}\text{O}$  and  $\delta^{13}\text{C}$ .

### 3. The Caiaphas Cave Tomb Ossaries: Microstratigraphy and Microfabric

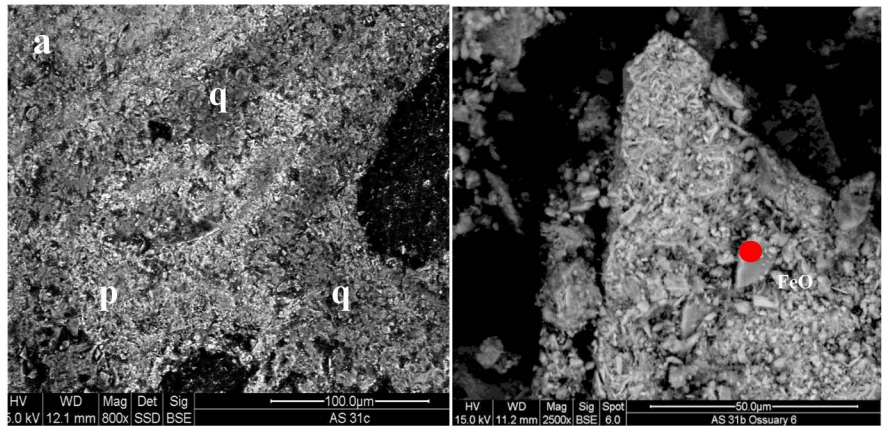
Burial tombs are cave-like features and the ossuaries therein act like small caves within a larger one. An ossuary is a box generally constructed of local stone, in Roman period Palestine soft local chalk and limestone were the favored construction materials. Ossuaries were the final resting place of human skeletal remains containing a single or occasionally more skeletons. During burial, a body was first placed on a temporary rock ledge inside the tomb from which, after about one year, the bones were removed and placed inside an ossuary. Besides the skeletal remains, natural materials inside tomb caves are weathered and disintegrated local stone to which varying amounts of soil and organic matter were subsequently contributed by the incursion of water during seasonal winter rains. Periodically, added to this mix was aerosol—a mix of wind-carried fine particles of comminuted rock (mostly well-polished quartz micro-grains) and soil with additions of local organic materials. Soils in major part develop by weathering of local bedrock, in West Jerusalem this is Turonian age limestone, dolomite and

more rarely clayey shales producing Terra Rossa soils. In South and East Jerusalem (the hill tops and eastward toward the Rift Valley) White Rendzina soils (Table 1, An. 41) overlie Senonian age chalk and chert bedrock. The specific location of the Caiaphas tomb ~50 meters directly downslope beneath the Hellenistic period Lower aqueduct, appears to have played a significant role in the geochemical evolution of the tomb and ossuaries by periodic contributions of moisture from water overflow in the aqueduct.

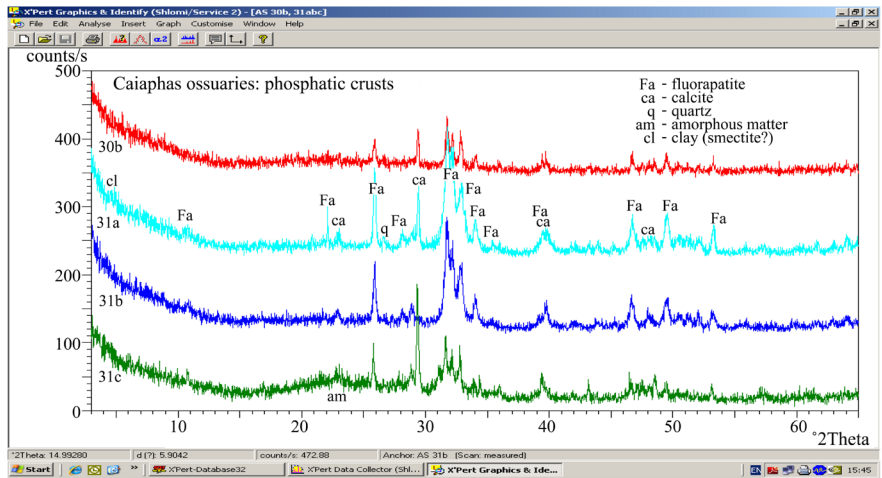


**Figure 2.** (a) Ossuary 6 interior vertical inner wall, showing the fine wall-parallel sedimentation laminae (a - e, details in text). (b) The inscribed and most decorated Ossuary 6, the two inscriptions—*Joseph son of Caiaphas* are on the left side and back face.

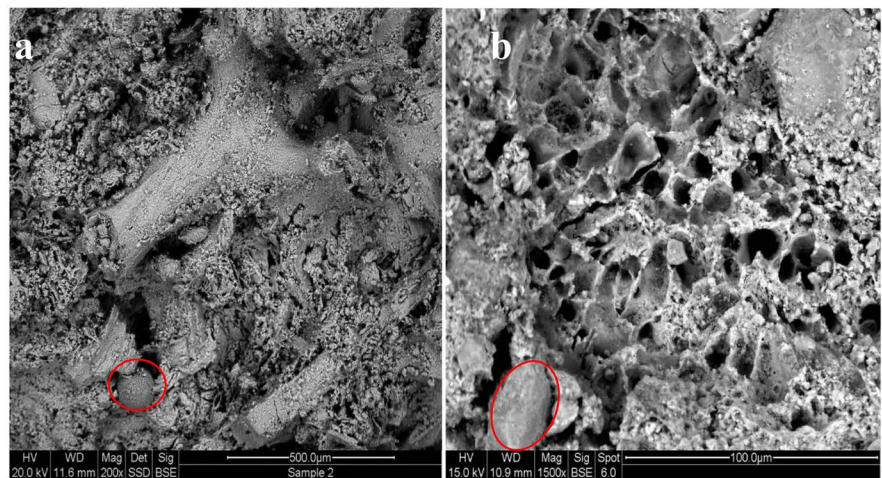
Optical microscope, and SEM examinations and eventually XRD analyses showed that much of the bone components in the ossuaries suffered degradation, micritization and recrystallization. For a climate entirely dry for about seven months of the year, more than the usual amount of moisture must have periodically entered the Cft ossuaries. This is well shown by a discreet wall and floor-parallel millimeters-thick internal lamination of fine sediment mixed with decayed bone rubble containing small amounts of other organic materials. It is particularly well manifested on the walls of Ossuary 6 (Figure 2(a)) as a white chalk (ossuary construction material) substratum (a) covered by a pale brown clayey soil layer (b) in turn covered by fine layers of lumpy phosphatic crusts (c) finally capped by a veneer of white carbonate flowstone carrying much aerosol quartzose dust (d). The vertical wall layers formed during fluctuating water level inside the ossuary and accretion onto the walls of fine sediment floating on the water interface. The ossuary floor (e) exhibits a similar horizontal micro-lamination with individual floor laminae of detritus carrying soil, micrograins of quartzose aerosol (Figure 3(a)), degraded bone and finally flowstone. Bone degradation was accompanied by crystallization of fluorapatite [ $\text{Ca}_5(\text{PO}_4)_3\text{F}$ , Table 1, Figure 4] and hydroxyapatite [ $\text{Ca}_5(\text{PO}_4)_3\text{OH}$ ]. Small grains of anhydrite, gypsum, barite and chips of iron oxide (Figure 3(b), Table 1, An. 12, 16) are also present.



**Figure 3.** (a) Ossuary 6 phosphatic wall crust with quartzose lenses (dark zones—q). Light-colored internal laminae (p) are mostly degraded bone. (b) Ossuary 6 bone rubble with occasional chips of iron oxide containing up to 83.55% FeO set in a matrix of quartzose dust and decayed bone. One possible source for such FeO-rich exotic fragments is nails placed in the ossuary.



**Figure 4.** X-ray diffraction (XRD) mineral composition of interior wall crusts in Ossuaries 3 and 6. The phosphatic crusts laminae contain mainly fluorapatite, quartz, calcite, clay minerals and amorphous (degraded and decayed) materials.



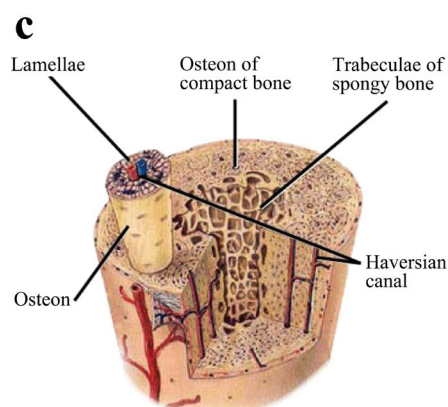


**Figure 5.** (a) Ossuary 6 bone rubble, the larger bone fragment is about 150  $\mu\text{m}$  in diameter, it may be a tiny rod-like fragment from a trabecula. The sphere beneath (marked) seems to have a hypha opening on the top, its size ( $\sim 80 \mu\text{m}$  diameter) suggests it may be a fungal sporangium (below) or fossil diatom. (b) Ossuary 1 degraded bone microstructures. The single oval grain (marked, lower left,  $\sim 50 \mu\text{m}$  long axis), is a typical aerosol quartz grain, such grains are ubiquitous in the tomb ossuaries and also adhering onto the two nails. The bone microfabric suggests this to be a fragment from a soft bone spongiosa. (c) Model of an osteon system and trabeculae of spongy bone. Source for (5c): <https://training.seer.cancer.gov/anatomy/skeletal/tissue.html>.

### 3.1. Botryoidal Microstructures

Under the optical microscope the phosphatic crusts (above) are seen as fibrous, variously degraded (optically opaque) bone tissue containing here and there discontinuous quartzose clusters and lenses (**Figure 3(a)**). The laminae are frequently packed with concentrically zoned spheres, 10 - 40  $\mu\text{m}$  in diameter, seen as individuals, joined couplets or in the form of continuous films of what appear to be botryoidal forms (**Figure 6a**). The spheres consist of 3 - 4 outer concentric rings and an inner core of fibrous crystallites radiating around an opaque black carbon-rich core (**Table 1, An. 17, 18**). The surrounding cryptocrystalline remains of decayed bone tissue consist of fluorapatite with small amounts of fine quartz incorporated onto apatite micrograins and also as lenses and fine lamellae (**Figure 3(a), Table 1, An. 8 - 11**). We interpret the botryoidal biofilms of adhering spheres to be the result of bone decay due to microbial infestation responsible for the chemical dissolution of bone tissue. Some bone tissue has retained its bone microfabric and osteon rings with concentric lamellae (**Figure 5(c)** and **Table 1, An. 10, 11**) remain well preserved.

Besides degrading bone botryoidal structures are also common of certain types of iron oxides, goethite for example frequently grows in lumpy-botryoidal forms. In this case, they form when crystals grow radially around nuclei of specks of sand or dust culminating as microscopic but up to megascopic half-spheres. Such structures are also pronounced features of carbonate flowstone. In the present case, we demonstrate their presence in Ossuary 6 but also as oxidized iron of Nails 1 and 2. The chemistry of the laminated Fe-hydroxide botryoids reveals somewhat low FeO contents but high concentrations of what may be organic carbon (**Table 1, An. 30 - 32**) thereby implying microbial activity (below).

**Table 1.** Chemical data for morphological structures in Cft Ossuaries and two Nails.

No.	Sample	Material-location	Element %							
			SiO <sub>2</sub>	Al <sub>2</sub> O <sub>3</sub>	FeO	CaO	MgO	P <sub>2</sub> O <sub>5</sub>	F	CO <sub>2</sub>
<b>Ossuary 3</b>										
1	AS30b	ossuary wall (sediment. veneer)	3.76	0.38	nd	11.63	0.21	8.35	0.18	75.25
2	AS30b	ossuary wall crust	3.12	0.42	nd	27.25	0.25	19.95	0.38	48.28
3	AS30b	ossuary wall (grey-fibrous zone)	1.96	0.3	nd	23.11	0.33	16.69	0.18	57.04
4	AS30b	ossuary wall, sed. substratum-o	7.72	2.86	1.05	20.82	0.74	2.26	nd	63.61
5	AS30b	ossuary wall, sed. substratum-i	8.4	3.18	1.27	20.99	0.59	2.27	nd	20.99
6	AS30a	ossuary floor, red crust	3.85	1.19	nd	27.24	nd	21.19	nd	46.53
7	AS30a	ossuary floor, brown crust	6.16	2.58	1.74	49.68	0.4	24.76	nd	14.67
<b>Ossuary 6</b>										
8	AS31a	ossuary wall, accretion rim	9.84	nd	nd	52.25	0.8	2.8	nd	34.31
9	AS31a	inner phosphatic zone (p)	6.55	nd	nd	42.92	nd	30.63	nd	nd
10	AS31a-1	outer quartzose lamella (q)	70.22	nd	nd	5.23	nd	nd	nd	24.55
11	AS31c	ossuary wall crust-osteon rim	10.07	0.11	nd	20.07	0.17	14.65	nd	54.63
12	AS31b	ossuary floor, Fe-rich fragment	3.61	nd	79.69	11.01	nd	5.7	nd	nd
13	AS31b	spore cluster in wood cell	nd	nd	nd	49.72	nd	30.74	nd	19.4
14	AS31b	wood cell wall	nd	nd	nd	44.58	nd	32,17	nd	22.73
15	AS31b	spheroid, germinated spore?	20.17	0.83	nd	36.1	nd	24.46	nd	18.44
16	AS31a	ossuary floor, Fe-rich fragment	1.37	nd	83.55	9.17	nd	5.91	nd	nd
17	AS31a	botryoid, outer lamellae (O)	2.97	nd	nd	29.42	nd	22.25	nd	45.36
18	AS31a	botryoid, fibers in core (i)	1.24	nd	nd	18.17	nd	13.67	nd	66.92
19	AS-X	Insect, interior skin fabric	0.34	1.4	nd	0.84	0.2	0.5	nd	96.72
<b>Ossuary 7</b>										
20	AS47	hypha in biofilm	4.57	2.9	0.89	41.08	0.54	4.18	0.73	44.97
21	AS48	germinated spore in biofilm	1.89	2	0.93	41.48	nd	27.39	0.73	25.56
22	AS48	brown crust, spheroid in biofilm	3.46	2.65	1.07	39.48	nd	24.39	0.66	28.29
23	AS48	floor, brown crust, hypha tube	5.55	2.56	1.67	41.01	nd	16.34	0.68	32.2
<b>Ossuary 1</b>										
24	AS40a	floor crust-germ. spore	27.15	0.81	1.07	30.5	0.31	16.5	nd	23.44
25	AS40e	floor crust	4.88	2.11	1.1	36.66	0.97	20.91	0.77	31.22
26	AS41a	Floor-carb. flowstone	2.39	1.28	1.28	54.99	0.38	0.8	nd	38.55
27	AS42a	ossuary wall-outer crust	1.72	1.16	0.91	45.28	nd	22.98	nd	27.96
<b>Nails</b>										
28	Nail 1	Crystallites-magnetite	0.78	nd	35.8	nd	nd	nd	nd	63.48
29	"	crystallites, carb. substratum	0.37	nd	4.85	14.05	0.76	nd	nd	79.98
30	"	dark brown Fe-oxides	2.54	nd	23.57	0.51	0.36	nd	nd	73.01
31	"	red Fe-oxides	1.55	nd	27.1	0.36	0.28	nd	nd	70.7
32	"	FeO botryoid	1.36	nd	20.19	0.33	0.19	nd	nd	77.93
33	"	wood, cell wall	2.68	3.01	64.1	1.55	0.53	nd	nd	27.87
34	"	germinated spore in tracheid	4.98	0.8	57.6	2.23	0.47	nd	nd	33.92
35	"	micro-bone fragment	1.16	1.54	90.6	1.83	nd	nd	nd	4.87
36	Nail 2	fibrous crystals cluster	1.17	0.57	7.99	14.9	0.37	0.57	nd	74.14
37	"	plumose crystals cluster	0.04	0.62	20.75	12.14	0.3	0.23	nd	65.02

## Continued

38	“	plumose crystals cluster	0.95	nd	54.61	0.42	nd	nd	nd	44.02
39	“	micro-bone fragment	5.18	0.46	70.4	6.18	1.01	nd	nd	16.77
40	“	aerosol quartz grain	41.76	13.92	15.01	3.06	0.53	nd	nd	21.96
41	“	Talpiot Hill Rendzina soil	11.77	3.4	1.45	31.08	0.71	1.15	nd	nd

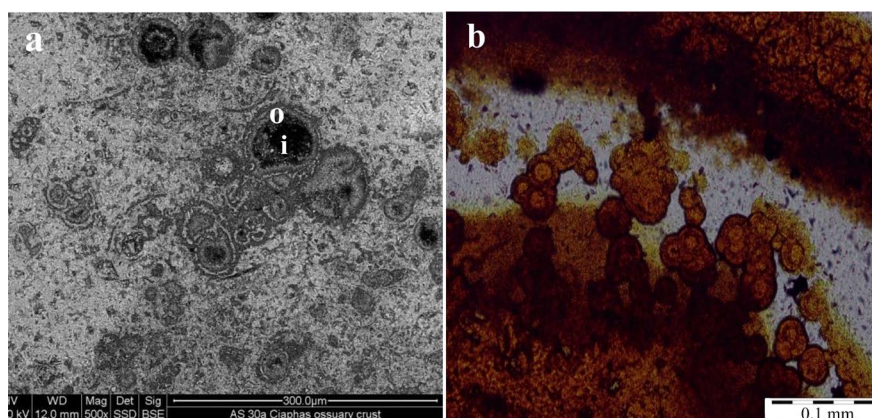


**Figure 6.** Botryoidal microstructures. (a) Clusters of spheroids resulting from microbial activity in bone debris. The spheroids are phosphatic botryoids, concentrically zoned with an opaque core rich in carbon (o - i, [Table 1, An. 17, 18](#)). (b) Laminated and botryoidal Fe-hydroxide in Nail 1 ([Table 1, An. 30 - 32](#)). Transmitted light optical microscope micrographs.

### 3.2. Carbonate Flowstone: Accretion Fringes

Accretion fringes are minor but important microstructures in the ossuaries. They are seen as fine laminae mantling clasts of quartz and bone fragments in Ossuary 6 and also as carbonate mantles around fragments of laminated iron oxides of the nails. The microcrystalline fringes are ~0.05 to 0.1 mm (50 - 100 um) in diameter, in Ossuary 6 they consist of two discreet laminae ([Figure 7\(f\)](#)) both of calcite with up to 10% quartzose dust ([Table 1, An. 8 - 10](#)) and traces of clays (Al +/- Mg), Mg-salts and bone (P + Ca). The carbonate flowstone is clearly visible as the lumpy—outermost lamina (d) in [Figure 2](#) and also as the white carbonate carapace covering segments of Nail 1 and Nail 2. The flowstone is important, besides providing us with important carbon-isotopic data, it seems to delineate an especially wet climatic period which affected the interior of all Caiaphas tomb ossuaries and the two unprovenanced nails at the same time. The carbonate fringes mantle quartz grains, bone fragments and other morphological elements in ossuaries and nails ([Figure 7](#)).

## 4. THE NAILS: Morphology and Mineralogy

We refer to the two nails studied as Nail 1 (white carbonate head) and Nail 2 (white carbonate lower body). The nails are 8 cm long with a slightly tapered end, they were purposely bent at an angle of 65°—on Nail 1 and 75°—on Nail 2 ([Figure 8](#)), a practice apparently linked to nails used in crucifixions. The white fragments attached to the Aba and Yehohanan nails (bottom right) are mostly

secondary phosphate minerals formed from the decay of bone phosphorus. The external crust of metallic iron of the nails is now entirely converted to micro-laminated orange to reddish-brown to almost black-colored iron hydroxides (**Figure 7(d)**). Some of the lamina are rich in concentrically zoned spheres (botryoids above) which, if organic in origin (**Table 1, An. 30 - 32**) may suggest that bacterial Fe (II) oxidation by (iron-eating) microorganisms (**Casanova et al., 2010**) may have played a role in the conversion of metallic iron to iron oxide. We emphasize that amongst the phosphatic floor debris of Ossuaries 6 and Ossuary 1 we found a number of fine chips of iron oxide with FeO concentrations reaching 83.5% (**Figure 3(b)** and **Table 1, An. 12, 16**).

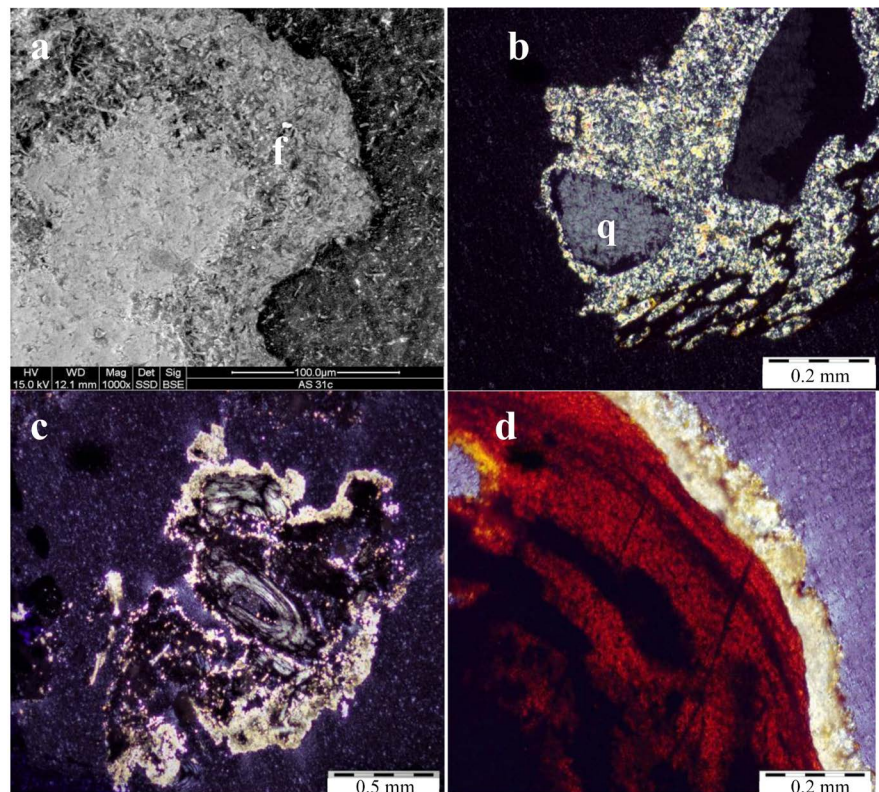


**Figure 7.** Accretion fringes of flowstone with quartzose aerosol. (a) Fringe (f) in Ossuary 6 wall crust and (b) mantling quartz grains (q) in floor rubble (one grain is black as it is in the extinction position), (c) fragment of bone osteon with concentric lamellae (**Figure 5(c)**) and (d) a fragment of microlaminated Fe-hydroxides from Nail 1. The color fringes are all carbonate flowstone ~80 - 250  $\mu\text{m}$  thick, some (e. g. f) with a quartzose inner segment (a) SEM micrograph. (b - d) transmitted light optical microscope images.

Fine fragments of iron oxide and separately from flowstone carapace were scrapped off the nail surfaces and studied under the optical transmitted light microscope, SEM and by XRD. During oxidation of the nails, the metallic iron was converted to finely laminated brown to reddish colored iron hydroxides goethite ( $\alpha$  goethite) and the uncommon lepidocrocite, a dimorphous form of goethite ( $\gamma$  goethite, **Figure 9**), both with the chemical composition  $\text{FeO}(\text{OH})$ . Although the amount of lepidocrocite is close to equal on the two nails the goe-

thite polymorph comprises ~44% on Nail 1 (white head) and ~67% on Nail 2. A small amount (~1.6%) of magnetite crystallites are present on Nail 1 but are not present on Nail 2 (**Figure 10(a)**, **Table 1 An. 28, 29**). The magnetite is present in perfectly shaped rhombic dodecahedra and cubes ~4  $\mu\text{m}$  in size; the crystallites define the final phase of iron oxide crystallization on the nails. In contrast to the hydroxides lepidocrocite and goethite the late-stage magnetite ( $\text{Fe}_3\text{O}_4$ ) crystallized in what, at that time, was an anhydrous environment.



**Figure 8.** Nails used in crucifixions. Nail 1 is bent  $65^\circ$  and Nail 2 about  $75^\circ$  at the broken tapered end. Slivers of (light colored) bone are attached to the Aba nail and the Yehohanan Heel Bone nail. The white carapace on the Caiaphas nails is calcite ( $\text{CaCO}_3$ ) flowstone. All the nails contain some adhered or perforated remains of bone tissue.

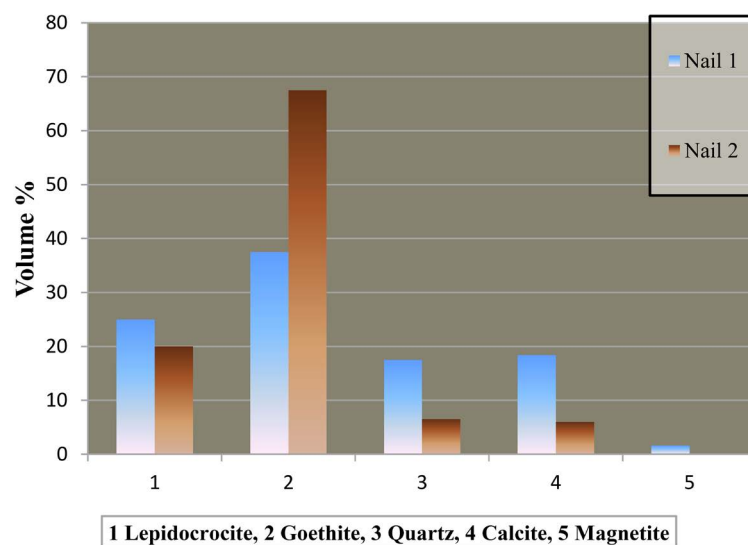


**Figure 9.** Column diagram for the main mineral constituents in the tomb Nails 1 and 2 (XRD determinations). Nail 1 was probably derived from Ossuary 1, Nail 2 from Ossuary 6.

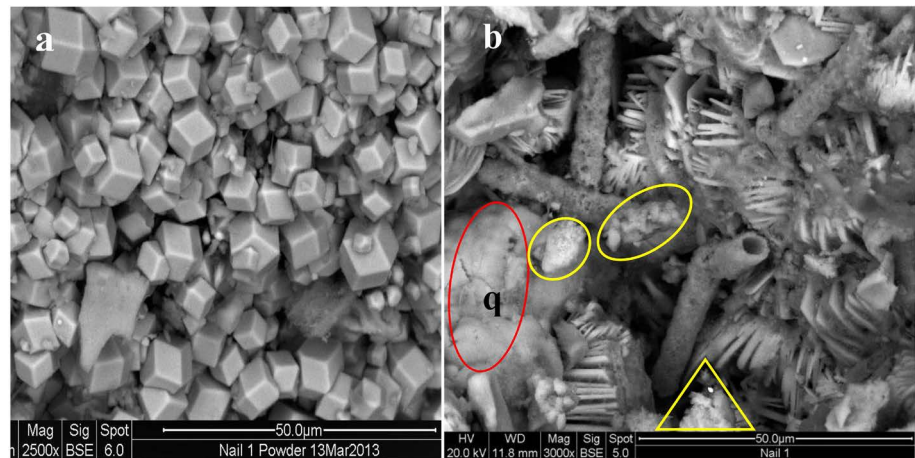


**Figure 10.** (a) Magnetite crystallites on Nail 1, the  $\sim 5\ \mu\text{m}$  size idiomorphic cubes and dodecahedra represent the final stage of iron oxide crystallization on the nails. It postdates flowstone deposition. The formation of magnetite crystallites may possibly be linked to a type of microbial activity responsible for biofilms seen in 10(b). (b) Fungal filament tubes (hyphae) set in a mass of plumose lepidocrocite crystallites and aerosol quartz (q) in Nail 1. Three bundles (yellow marked) of small spores appear to be encapsulated in transparent (bacterial?) biofilms.

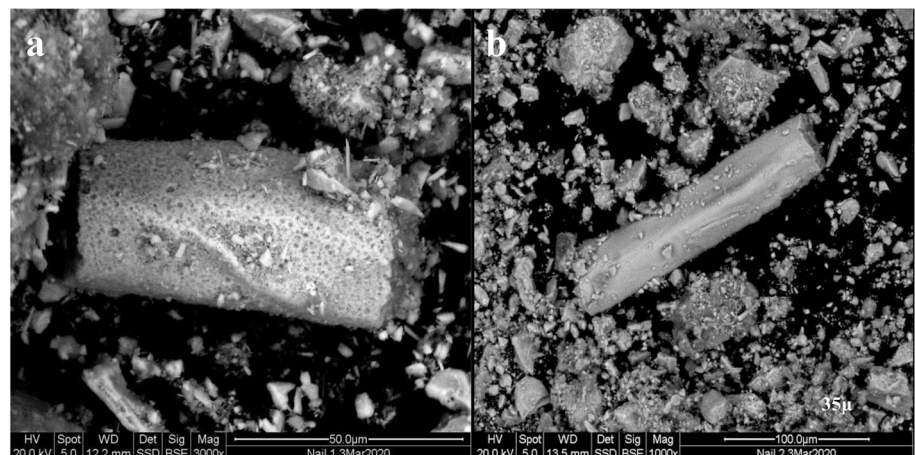


**Figure 11.** Micro-bone fragments in the rubble of Nail 1 (a) and Nail 2 (b). The bones are tiny and may be segments of what was spongy bone tissue in an osteon system (e.g. rod trabeculae, **Figure 5(a)**, **Figure 5(c)**). Both of what were phosphatic bone fragments are now entirely composed of Fe-hydroxides (**Table 1 An. 35, 39**).

## 5. The Wood: Micromorphologies and Determination of Wood Type

We were amazed to discover, even under low power SEM magnification,  $\sim 2\ \text{cm}$  long fine slivers of wood accreted to both nails buried within quartzose sedimentary debris. Many of the wood cells are entirely filled with radiating fibers and blades of crystalline iron hydroxides (**Figure 13(a)**). In addition, we also found in the ferruginous debris and within the wood tracheids (cells), small—yet very pronounced amounts of organic materials *all of which we have also identi-*

*fied in the tomb ossuaries.* They include chips of micro-bone, fungal sporangia, at least two dominant forms of spores and related filament tubes such as sporangiophores and hyphae (Figures 12-16). Near concentrations of organic debris we have noted (SEM-EDX) an occasional pronounced increase (0.2% - 0.57%) in phosphorus concentration (e.g. Table 1, An. 36, 37), a feature especially noted on Nail 2. We attribute such anomalous phosphorus concentrations to the presence of bone tissue now, as shown above, in major part decayed or replaced by iron oxides (Figure 11, Table 1 An. 35, 39). It is amazing how the organic components of the wood, including all the invasive and/or accreted biological species have, as the wood, been entirely converted to iron hydroxides. A similar phenomenon, a “pseudomorphous” replacement of coffin wood cells by iron corrosion products adjacent to iron bars inside an 8<sup>th</sup> century BC tomb at Gordion, Turkey, was observed by Blanchette and Simpson (1992). We consider such complete replacement of the wood organic components by iron hydroxides as a petrification process, in the sense that the mobile iron replacing the organic compounds was controlled by the wood and fungal microarchitecture on an atom by atom basis.

One of us (WHS) identified the wood to be that of a mature *Cedrus* (*Cedar*)—a genus of coniferous trees in the plant family Pinaceae. In the Mediterranean region Cedar occurs at altitudes of 1000 - 2200 m and although an important tree in the mountains of Lebanon (*Cedrus Libani*), Syria and Turkey it was a special and costly, perhaps even extraordinary, import into Roman period Palestine. The present identification is based on detailed SEM study of some well preserved morphological features which characterize Cedar wood. They include the width of latewood zones, decorated tori, rays of parenchyma cells with taxodioid pits, heterocellular rays and resin canals, features we show below (Figure 13, Figure 14, Figure 16(a)).

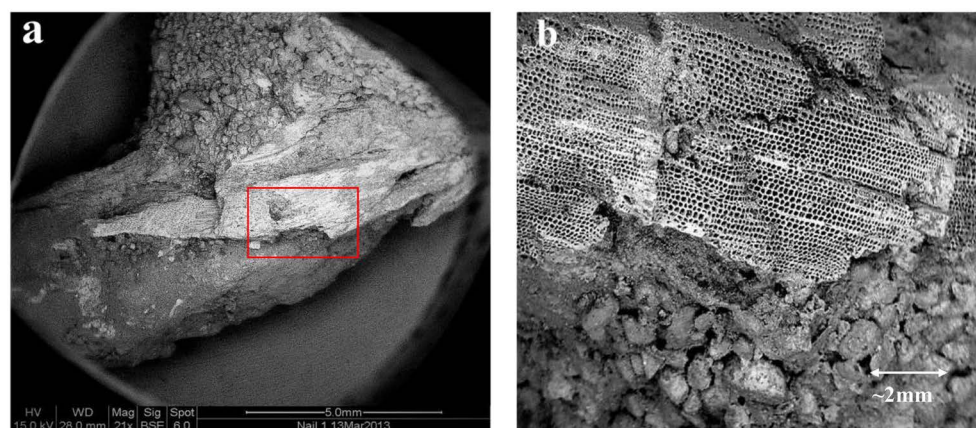


**Figure 12.** (a). Slivers of wood accreted to Nail 1 by Fe-hydroxides. Aerosol quartz (fine grains 150 - 300  $\mu\text{m}$  in size) with a clayey dust veneer is filling gaps between wood and nail Fe-hydroxides. (b) Detail on wood, the fine black dots are a transversal view of tracheids—the cellular microstructure of wood. The entire wood sliver (left photo) is about 2 cm long.

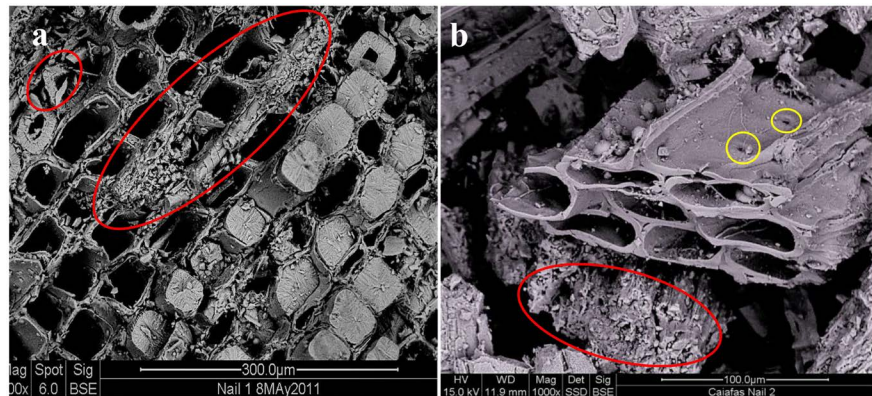


**Figure 13.** (a) Wood microfabric. Transverse view of wood sliver from Nail 1 reveals detail of tracheid cells many of which are entirely filled with radiating fibers of goethite (white). (b) Both transverse and tangential sections of tracheids. Large Sg spores inhabit a few cells some of which exhibit bordered pits (yellow markers). Many tracheids have suffered decay and total collapse (red markers) as a result of fungal attack and degradation processes. Fungal activity was either coeval with or postdates Fe-hydroxide crystallization inside the tracheids as some cells filled with crystallites are deformed.

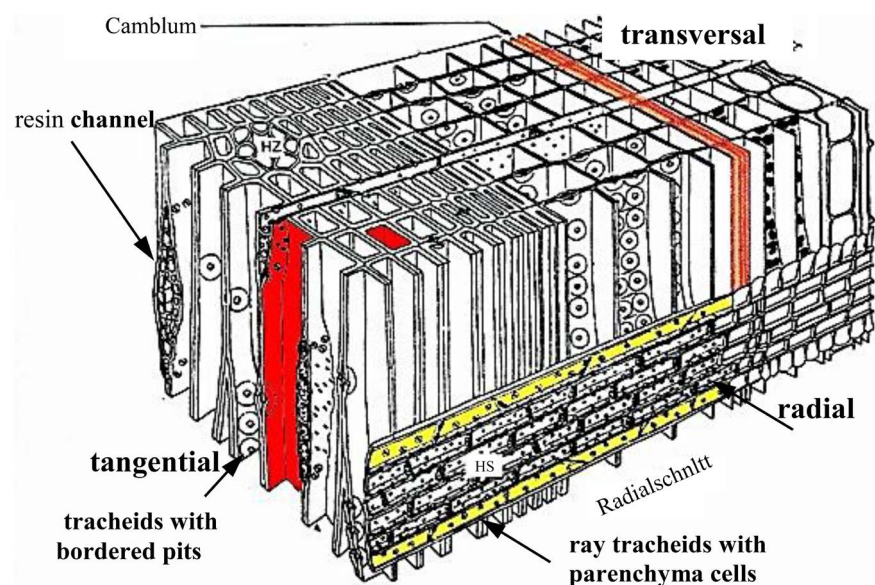


**Figure 14.** Model of wood cells with different perspectives of the main microstructural elements. Source: Timber Construction Material p. 31 after: “Magdefrau 1951”.

## 6. Bioinfestation: Microfauna and Microflora

During our study of the Caiaphas tomb ossuaries and the two unprovenanced nails we discovered evidence of widespread microbial infestation accompanied by partial biodeterioration of organic components in both the ossuaries (bones) and also of the wood accreted to the nails (above). Bone and wood provided a choice habitat for microbial attack and both were colonized by what appears to be a single species but it is feasible that in view of the ~1900 year time span, more than a single generation and species of fungi is manifested. The fungal morphologies include (Figures 15-17) round to occasionally oval microstruc-

tures most of which constitute fungal sporangia. The sporangia are enclosures in which spores—the fungal reproductive cells—are formed and from which they eventually are forcefully expelled before proceeding to the next evolutionary step of germination. The sporangia and germinating spores often exhibit protrusions of filamentous tubes (sporangiohores or hyphae)—the main mode of vegetative growth of fungi which function as conductors transporting water and other nourishment from roots to leafs of growing plants. The spores when released from their housing into the air are dispersed by wind and water and can travel great distances from their source.

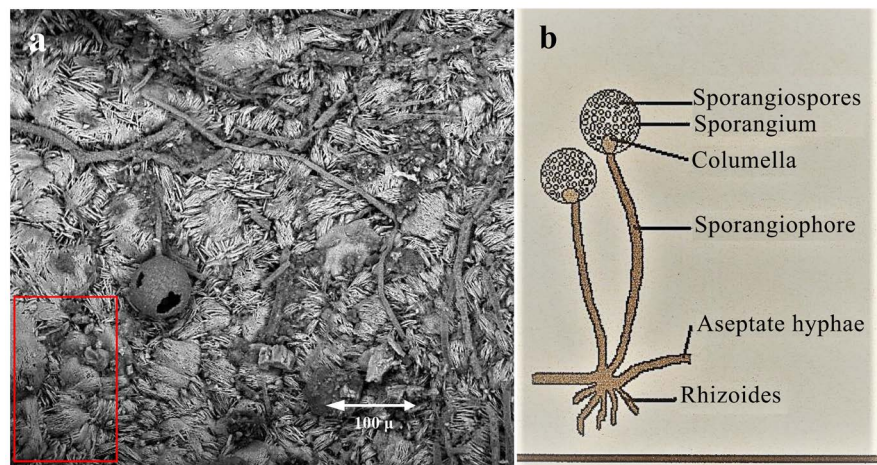


**Figure 15.** (a) Fungal sporangium with a protruding filament tube (sporangiohore). The surrounding crystalline matrix consists of bladed lepidocrocite +/- goethite and broken fungal hyphae. With the exception of a few fine grains of quartz (lower left) the whole mass is chemically iron hydroxide. (b) A model of the most basic of fungal morphologies. Source: <http://www.fungionline.org.uk/>.

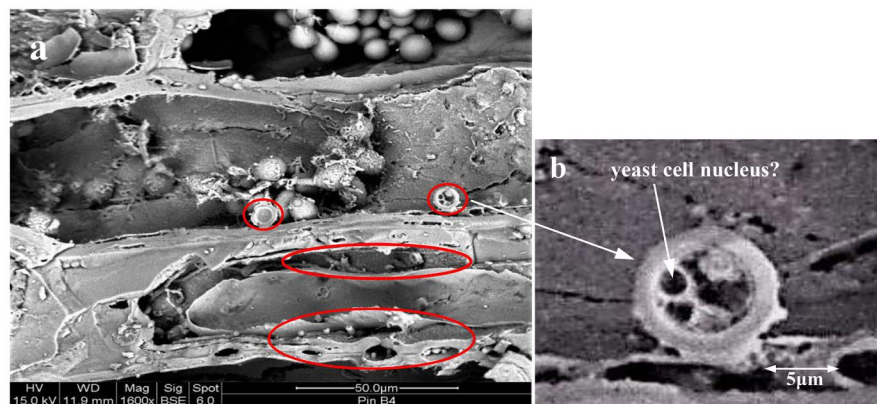


**Figure 16.** (a) Wood microfabric and microbial activity in Nail 2 wood tracheids (tangential section), note bordered resin pits some carrying discrete Ss spores and broken hyphae. Slightly conical Sg spores (~8 - 10 μm diameter) some with protruding hyphae are clustered in what we interpret as resin channels (Figure 14) that carried plasma in the form of sugar or starches. Some spores (marked) have concentric laminae, perhaps as layers of wall material added during germination. Others (b) exhibit an internal microstructure markedly similar to yeast cells.

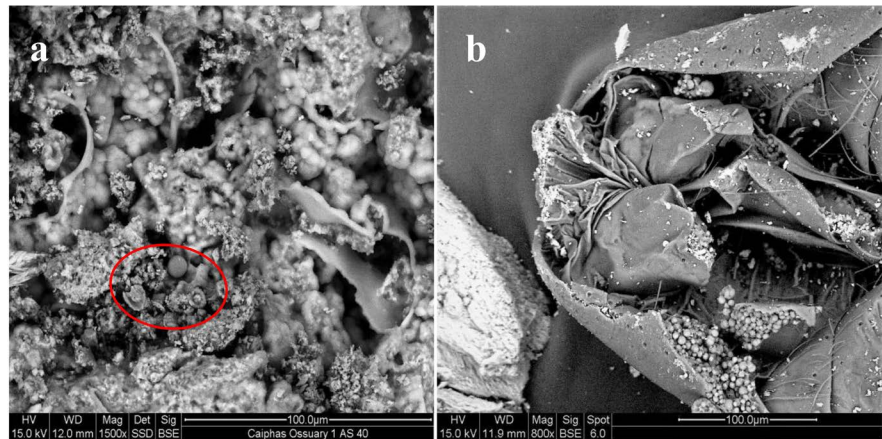


**Figure 17.** (a) Ossuary 1, degraded bone microfabric, the voids are filled with globular Ss spores. Enclosed spherical structures are foraminifera, one spheroid is an Sg spore or diatom (**Table 1 An. 24**). The bone microfabric may be trabecular spongiosa, a mixture of bone mineral and marrow. (b) Head (underside view) of an insect, possibly a Tube-Tailed Thrips. Although Thrips feed on fungal spores in the present case it seems that the spores had the advantage and colonized the insect's body. The insect is a late visitor as the body has retained all its carbon (**Table 1, An. 19**).

Fungal activity inside ossuaries will result in partial to complete degradation, or chemical breakdown, of bone microstructures and, if present, the wood cell network. In the latter case, decay attacks the primary cell wall components—the carbohydrates, lignin and cellulose, a process accompanied by the release of CO<sub>2</sub> (**Figure 13, Figure 19** and **Table 1, An. 33**). We have observed two (but not only) principal varieties of spores in our materials (1) a group of small spores ~3 to ~4 µm (0.003 to 0.004 mm) in size and (2) a second group ~8 to ~10 µm in size, with some marked exceptions (e.g. **Figure 19(b), Figure 20(a)**) noted. We will herewith refer to the former as Ss (small) spores and the latter as Sg (germinated) spores, the former (Ss spores) resemble a tightly clustered mass of globules or clusters of grapes, the latter (Sg spores) occur as individuals or small bunches of ~5 - 10, frequently pear-shaped bodies. The Ss spores are very much dominant inside the ossuaries where they have colonized the microstructures of bones but also other organic (e.g. insects, **Figure 17(b)**) morphologies. The Sg spores, although also present inside degraded bone microstructures, are ubiquitous inside the wood tracheids, which was clearly their much preferred habitat. Because of the close spacial relationship and presence of what appear to be transitional stages between the two spore groups (e.g. **Figure 19** and **Figure 20(a)**) we reason that rather than what at first glance appear to be different fungal species they are one species in different stages of development leading to germination. We emphasize that some of the spore-like structures reveal an internal microfabric resembling yeast cells (**Figure 16(b)**). Spores are unicellular, but under favourable conditions, which involves an exogeneous supply of moisture, water and nutrients will germinate, a process that entails spore swelling and change in shape and finally extrusion of one or more germ-tubes (**Figure 18(a)**,

**Figure 19(a)**). Microbial degradation is affected by amount of light, water and oxygen availability, it will take place as the hyphae spread through food and release enzymes that break food down into substances that the fungi can easily absorb. In **Figures 15-20**, we have tried to elucidate some of these processes and the range of fungal micromorphologies that we have encountered in the ossuaries and nails (Full explanations in: <http://www.fungionline.org.uk/>).

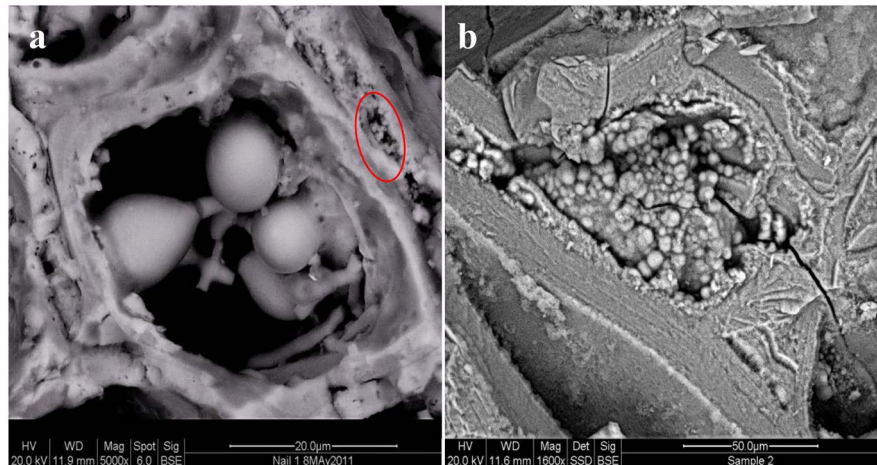


**Figure 18.** (a) Wood tracheids transversal sections in Nail 1 and (b) in a wood fragment in Ossuary 6. In (a) the cell is occupied by germinated-conical Sg spores, germ tubes protrude and bifurcate, they are attached to the cell walls from which nourishment is drawn. Small globular Ss spores in (b) have not germinated. The Sg spores in (a) and tracheid are compositionally Fe-hydroxide, in (b) spores and wood cell are bone apatite rich in P and Ca (**Table 1, An. 13, 14, 33, 34**).

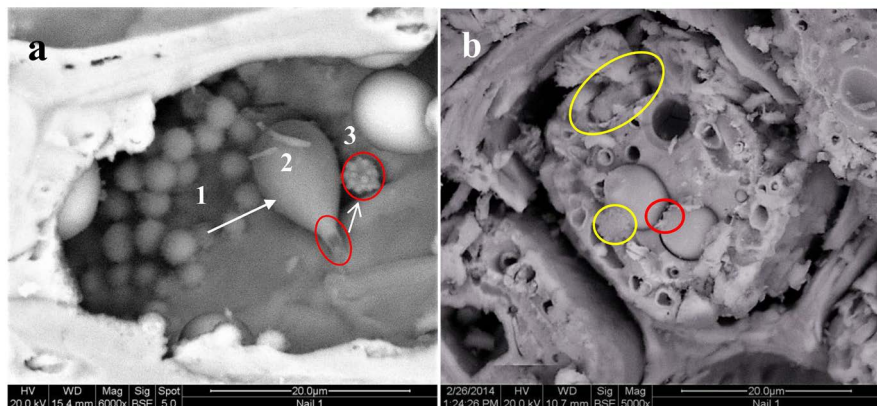


**Figure 19.** (a) The figure illustrates the link between the three principal morphological forms of what we view as evolving spores: (1) a cluster of small (Ss) spores, (2) a germinated Sg spore, it has swollen and is much larger than its predecessors, it is now cone-shaped with an emergent germ tube, (3) a small apical vesicular complex of fine cells (AVC) has broken off from the tube terminus. In (b) the full array of spore sizes is seen within a single tracheid, the spores range from  $\sim 2 \mu\text{m}$  to  $\sim 10 \mu\text{m}$ , they seem to be embedded in what was a soft tracheid resin. One large Sg spore shows an opening on the upper left surface (red marking). In yellow enclosures are spore clusters enveloped in biofilms (discussed below).

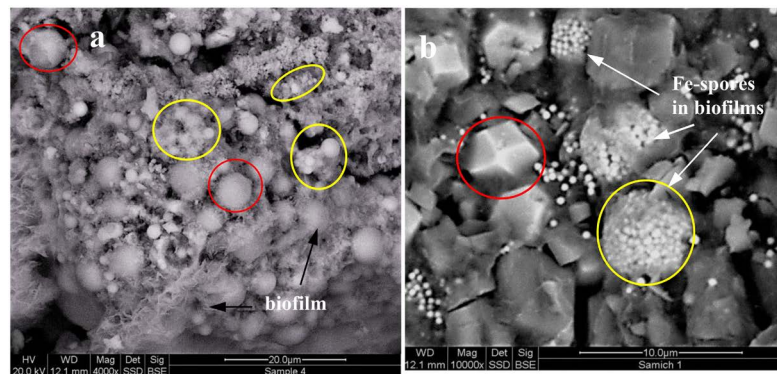


**Figure 20.** (a) Fungal chaos or fungal—bacterial coexistence in Ossuary 7. As in **Figure 19** (in wood) the full range of Ss, Sg (and bacterial?) spores (sizes  $< 1 \mu$  to  $\sim 8 \mu$ ) is exhibited. Some spore bundles, and the bottom right area, are enclosed by a veil-like biofilm, perhaps due to late bacterial attack—or possibly in a symbiotic relationship with the fungus. (b) Bacterial biofilms inside the surface patina of a construction stone, shown for comparison. Some Fe-spheres (white,  $\sim 1 \mu$ m in diameter) are scattered but also coalesced inside biofilms. The process culminated in crystallization of idiomorphic pyrite dodecahedra ( $\text{FeS}_2$  marked) and cubes. We point out that the latter are not unlike the magnetite crystallites in Nail 1 (**Figure 14(b)**). (**Figure 20(b)** from Shimron, A. E. 2012, unpublished report).

### 7. $\delta^{18}\text{O}$ and $\delta^{13}\text{C}$ Isotopes of Ossuary 6 and Nail 1 Speleothems

Surface rain waters percolate downward through soil and by reacting with  $\text{CO}_2$  supplied by biological activity form carbonic acid ( $\text{H}_2\text{CO}_3$ ). The acid reacts with the host rock and the water becomes saturated with respect to calcite forming  $\text{Ca}(\text{HCO}_3)_2$  in solution. Should the water reach the open space of caves (or tombs) under certain conditions  $\text{CO}_2$  degassing will take place and carbonate minerals will be deposited as speleothems or flowstone (stalactites, stalagmites). Chemically what takes place is the compound  $\text{Ca}(\text{HCO}_3)_2$  breaks up to  $\text{CaCO}_3$  (flowstone) +  $\text{CO}_2$  +  $\text{H}_2\text{O}$ . In their study of some Israeli caves **Bar-Matthews & Ayalon (2001, 2004)** amongst others, have shown that the oxygen isotopic composition ( $\delta^{18}\text{O}$ ) of speleothems reflects the temperature at the time of their deposition and also the  $\delta^{18}\text{O}$  values of the water from which they were deposited. In another study, performed to evaluate the rain shadow effect on the amount of rainfall and speleothem growth, **Vaks (et al., 2003)** found that variations in the carbon isotopic composition ( $\delta^{13}\text{C}$ ) of speleothems results from differences in the type of vegetation in the vicinity of the cave. In such a case, enrichment in the  $\delta^{13}\text{C}$  (seen in lower negative values) of calcite speleothems usually reflects an increase in the contribution of C4-type plants (crop plants, saltbush, corn, annual summer plants) to the soil  $\text{CO}_2$ . We know that the sudden passage from the western to the eastern (rain-shadow) side of the Jerusalem mountain ridge is highlighted by an increase in temperature and evaporation rates, in addition to being accompanied by a sharp drop in rainfall from  $\sim 500$  to 250 mm (**Vaks et al., Figure 1**). Notably, these features are also manifested by an increase in  $\delta^{18}\text{O}$  and  $\delta^{13}\text{C}$  (lower negative) values. On the basis of these data, it has been concluded

that the  $\delta^{18}\text{O}$  and  $\delta^{13}\text{C}$  isotopic composition of speleothems is dependent on environmental conditions.

The Ma'ale Efrayim Cave is located in the rain shadow on the eastern side of the central mountain ridge on which Jerusalem is located. The Soreq Cave is located in the rainier western side of the mountain ridge whereas the Jerusalem West Cave (Frumkin et al., 1999) lies close to the central part of the ridge, near the heart of the city. The Caiaphas family tomb lies about 7 km directly south of the Jerusalem West cave about halfway between central Jerusalem and Bethlehem. It is located on the east-facing slope of the Jerusalem mountain ridge, just within the western edge of the “rain shadow” desert region (ref. above). We show and compare our  $\delta^{18}\text{O}$  and  $\delta^{13}\text{C}$  values with data from flowstone collected from the caves above (Table 2, Figure 21). We note that the  $\delta^{18}\text{O}$  and  $\delta^{13}\text{C}$  values we obtained for Ossuary 6 and Nail 1 are (1) very similar and (2) considerably closer in magnitude than values obtained from the same speleothem for different periods in time in the caves above. The Nail 1 value is close to Jerusalem West cave present values. Isotopic  $\delta^{18}\text{O}$  and  $\delta^{13}\text{C}$  values oscillate frequently with time and up to 2.15‰ variation within a single annual growth band has been measured, consequently, the small difference in the isotopic values of Nail 1 and Ossuary 6 is insignificant and can be attributed to a slight difference in time of speleothem deposition. We conclude that our  $\delta^{18}\text{O}$  and  $\delta^{13}\text{C}$  values are 1) higher than almost all values for the last ~5000 years obtained for flowstone from Jerusalem area caves and 2) it appears that waters from an area rich in C4-type plants made a higher contribution to the Caiaphas tomb and Nail 1 isotopic values than those from other caves sampled. Such data make the Ossuary 6 and Nail 1 values unique.

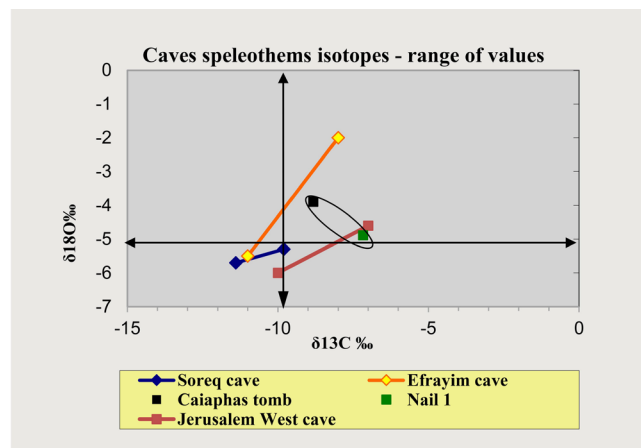


**Figure 21.**  $\delta^{18}\text{O}$  and  $\delta^{13}\text{C}$  isotope values for Ossuary 6 and Nail 1 with isotope values for speleothems from some Jerusalem area caves added for comparison. Jerusalem West data from Frumkin et al. (1999), Soreq and Efrayim caves data from Vaks (et al., 2003) and data for the Soreq cave from Bar-Matthews and Ayalon (2004). With the exception of one value for the Jerusalem West cave and one for the Efrayim cave the isotope values for Ossuary 6 and Nail 1 stand out as (1) being very similar and (2) higher (lower negative) from most other cave values in the Jerusalem area. With this in mind, the Ossuary 6  $\delta^{18}\text{O}$  is slightly heavier than is usual for Jerusalem (although within normal fluctuations) whereas the  $\delta^{13}\text{C}$  is a common Holocene value for this area.

**Table 2.**  $\delta^{18}\text{O}$  and  $\delta^{13}\text{C}$  isotope values for flowstone from the Caiaphas tomb, Nail 1 and for the Soreq, Efrayim and Jerusalem West caves.

Isotopes	Soreq Cave	Efrayim Cave	Jerusalem West Cave	Caiaphas Tomb	Nail 1
	West Judea hills	Jordan Rift valley	West Jerusalem	East Jerusalem	Caiaphas tomb (?)
$\delta^{18}\text{O}$ ( $\delta^{18}\text{O}$ )	-5.7 to -5.3‰	-5.5 to -2.0‰	-6.0 to -4.6‰	-3.9‰	-4.89‰
$\delta^{13}\text{C}$ (range)	-11.4 to -9.8‰	-11.0 to -8.0‰	-10 to -7‰	-8.82‰	-7.17‰
Period/time represented	Last ~5000 years	67,000 to 24,000 yr B.P.	Last ~3000 years	1 <sup>st</sup> century CE to present	1 <sup>st</sup> century CE to present

## 8. Discussion

**The Ossuaries:** The IAA has not reported two nails found or missing from any excavation other than those from the Caiaphas tomb. Nonetheless, we have examined the possibility that the unprovenanced nails were derived from another tomb where bioactivity by species identical or similar to those in the Caiaphas tomb had taken place. For this and other objectives, we have sampled and studied the petrography and petrochemistry of materials from interiors of about 40 ossuaries collected from some 25 tombs in the Jerusalem area (Shimron et al., 2020, Figure 1). We can now conclude that we have not found any fungal or bacterial species or biodegradation of the type we observed in the Cft and on the two nails, in ossuaries from any other tomb. In addition, neither have we found evidence or any record of such profuse and continuous flooding of ossuaries from any of the other tombs that we have examined. We reason that a continuous abundance of water and colonization of the tomb by a unique fungal species makes the Cft and materials found therein so profoundly unique. Besides winter rains the amount of moisture in the Cft was influenced by periodic water overflow from the neighboring Hellenistic period aqueduct. Wall-parallel laminae of sediment and bone rubble with various degrees of bone degradation and decay are testimony that geological and biochemical processes were periodically active in the ossuaries. The stone boxes with bones, two with oxidizing iron nails with attached wood in standing pools of water must have been magnets for robust fungal activity. Bone degradation, wood decay and the character of the nails' Fe-oxidation products testify on the dependence of their immediate environment on the amount and pH of standing water. We have shown that changes in bone micro-architecture seen in fragments of phosphatic crusts attached to the walls and floors of the ossuaries exhibit various stages of degradation, decay and recrystallization to fluorapatite [ $\text{Ca}_5(\text{PO}_4)_3\text{F}$ ] and hydroxyapatite [ $\text{Ca}_5(\text{PO}_4)_3\text{OH}$ ]—the expected and thermodynamically stable phosphate minerals that form under ordinary cave conditions (Trueman et al., 2004 and Table 1).

Although Ossuary 6 was found in situ, its cover was removed by Byzantine-period tomb robbers only to be replaced shortly thereafter perhaps out of respect for the recognizable inscribed Caiaphas family name. The ossuary was not moved by robbers from its original site for the same reason and the only disturbance it may have suffered is the removal and immediate disposal of a nail

(Nail 2) found by excavators on the kokh floor near the ossuary. In the first excavation report the head excavator (Greenhut, 1992) notes that “one nail was found inside one of the ossuaries” while the other on the floor of Kokh IV (that is near Ossuary 6). In a subsequent report Greenhut (2004) however notes that one nail (Nail 1) was found in Ossuary 1. In the present work, we have assumed that the latter report is accurate and that indeed one of the two nails (Nail 2) was removed from Ossuary 6 during the robbers’ incursion into the tomb whereas the second nail (Nail 1) spent its entire ~1900 year long history undisturbed inside Ossuary 1. We have summarized our main observations and elucidate the main links between the Cft ossuaries and the two nails in Table 3 below.

**Table 3.** Summary of the main events affecting Ossuaries 1, 6 and two unprovenanced nails.

Time-Period	Ossuary 6 (decorated)	Ossuary 1	Nail 2 (white cap) In Ossuary 6	Nail 1 (white body) In Ossuary 1
1 <sup>st</sup> century CE	Bones placed in ossuary  Intrusion of moisture. Bone degradation	Bones placed in ossuary  Intrusion of moisture. Bone degradation	Nail 2 placed in Ossuary 6  Nail metallic iron oxidation	Nail 1 placed in Ossuary 1  Nail metallic iron oxidation
	Incursion of water with aerosol and flooding of ossuaries. Brown base laminae deposited	Incursion of water with aerosol and flooding of ossuaries. Brown base laminae deposited	Fe-oxidation and crystallization of lepidocrocite. Fibrous goethite forms in wood cells.	Fe-oxidation and crystallization of lepidocrocite. Fibrous goethite forms in wood cells
1 <sup>st</sup> century CE Start of fungal infestation?	Microbial (fungal) activity, formation of phosphatic crusts on floor and walls of ossuary. Phosphatic botryoids	Microbial (fungal) activity, formation of phosphatic crusts on floor and walls of ossuary. Phosphatic botryoids	Microbial activity in wood cells, germ. of Sg spores, cell decay. Lepidocrocite and goethite. Bacterial activity, Fe-botryoids	Microbial activity in wood cells, germ. of Sg spores, cell decay. Lepidocrocite and goethite. Bacterial activity, Fe-botryoids
4-5 <sup>th</sup> century CE Byzantine incursion by tomb robbers	Ossuary uncovered, Nail 2 is removed from ossuary by tomb robbers and dumped on tomb floor. Ossuary lid is replaced	Ossuary moved from its kokh, lid is removed, ransacked by tomb robbers	Nail 2 is dumped on tomb floor. Fe-petrification of wood and fungi. Mostly goethite crystallizing on moist tomb floor at pH 7 or greater.	Fe-petrification of wood and fungi. <i>Lepidocrocite</i> is now the main Fe crystallizing (at pH 5 - 6.3) on ossuary floor.
The “Wet Event” inside the Cft	Deposition of flowstone crusts. CaCO <sub>3</sub> accretion rims	Deposition of flowstone crusts. CaCO <sub>3</sub> accretion rims	Deposition of flowstone crusts, CaCO <sub>3</sub> accretion rims	Deposition of flowstone crusts, CaCO <sub>3</sub> accretion rims
19 <sup>th</sup> -20 <sup>th</sup> century (bacterial activity?)	Bone degradation	Bacterial attack on Ossuary 7 fungal colony. Formation of biofilms in Ossuary 7 and Nail 1.	Bone degradation	Bacterial attack on Nail 1 fungal colony. Formation of biofilms and biocrystallation of magnetite above flowstone laminae

**The Nails:** The two iron oxydation products we have identified are goethite [ $\alpha$ -FeO(OH)] and lepidocrocite [ $\gamma$ -FeO(OH)]—the less stable and infrequently encountered polymorph of goethite. The reddish brown lepidocrocite (e.g. Figure 6(d)) crystallizes preferably when iron oxidizes in water under hydromorphic conditions in an anaerobic environment (Ross & Wang, 1982; Schwertmann & Taylor, 1972), but it has also been identified in association with biotic reactions that form iron-oxides (Schieber & Glamoclija, 2007). Its growth is in-

fluenced by a number of factors amongst which are a preferred pH between 5 and 7 and the presence of elements like phosphorus (Cumplido et al., 2000). Hydromorphic soils have a notably low pH of ~4.5 - 5, they are typical of marshes and bogs, a situation not unlike that prevailing in standing pools of water inside a tomb, or an ossuary with degrading and decaying bones infested by a fungal colony. The rubble in Ossuary 6 contains 0.8% and in Ossuary 1 and Ossuary 7 0.2% sulphur with locally up to 3% present. Such acidifying material lowers the pH of the waters which must already have been de-oxygenated by microorganisms feeding on organic material. In this manner, conditions were generated, in the tomb and ossuaries in which iron-oxidizing organism (which prefer to colonize in the transition zone between the anaerobic and aerobic environments) thrive.

Although the two nails contain close to the same amount of lepidocrocite (~20% and 24%, **Figure 9**) the amount of goethite in Nail 2 is close to double that in Nail 1. This fact indicates that at some point in their history the geochemical setting of the nails must have changed in a manner that promoted the crystallization of goethite rather than lepidocrocite on Nail 2. Such a change in the geochemical milieu would have taken place when Nail 2 was removed from its Ossuary 6 habitat and dumped on the tomb floor by robbers during the Byzantine (4<sup>th</sup>-6<sup>th</sup> century CE) period. Conditions of light, temperature, pH and amount of water must all have changed for Nail 2 at this time. Any major influx of fresh water into the tomb would have resulted in improved oxygenation and a rise in the pH of tomb moisture. It is precisely this kind of change that is now manifested by the considerable dominance of goethite over lepidocrocite on Nail 2, an indication that their evolutionary paths must have diverged at about this time. Casanova (et al., 2010) showed that at pH 7 both lepidocrocite and goethite may form by Fe (II)-oxidizing bacteria whereas at pH lower than 6 lepidocrocite will be the favored iron oxide (a chemical condition also favouring yeast fungi). In such a case goethite, which is more abundant on Nail 2, crystallized in moisture with a pH near neutral or alkaline (pH 7 or higher). Such a change would have taken place had Nail 2 been removed from what must have been its initial hydromorphic-hypoxic environment (e.g. Schwertmann & Taylor, 1972) inside Ossuary 6 and transferred to a better oxygenated chemical environment on the tomb floor. Such an explanation is consistent with the archaeological findings and mineralogy of the nails. Evidence of a late change in the microbial setting of the nails is indicated by the presence of a small amount of the anhydrous iron oxide magnetite (Fe<sub>3</sub>O<sub>4</sub>, **Figure 10(b)**). Identified by SEM and XRD on Nail 1 these amazing ~5 µm size idiomorphic crystallites occur in clusters covering what is late-crystallized flowstone carbonate (e.g. **Figure 6**, **Figure 10(b)**, **Figure 20(b)**). The presence of such magnetite implies crystallization under hypoxic or anaerobic conditions during which the Fe-hydroxides can be further oxidized by organisms to form crystalline magnetite (Kirschvink et al., 1992; Lowenstam, 1981) which, it appears, became the thermodynamically more stable phase. The

magnetite clearly designates the final phase of iron oxide crystallization under what must have been anhydrous, possibly toxic, conditions.

**Bioinfestation:** The fungal spores must have arrived in the Caiaphas tomb mixed with atmospheric (aerosol) dust with quartz and clayey soil particles ubiquitous inside the ossuaries and also on the nails. The infiltration into the ossuaries of fine sediment carrying spores most likely took place during the intrusion of large amounts of water which periodically flooded the tomb. Fungi are heterotrophic organisms which cannot produce their own food instead they take nutrition from other organic sources such as bone or wood. Living bone consists of three major components, organic matter (mainly protein), mineral in the form of calcium phosphate (apatite), and water. Wood on the other hand consists primarily of cellulose—a form of carbohydrates, the primary target of fungi which metabolize the wood, resulting in carbon dioxide being released back into the atmosphere.

Some spore-forming bacteria can form highly organized multicellular communities referred to as biofilms (also called slime). Biofilms are one of the more extraordinary morphologies we discovered in the rubble of Ossuary 7 and also Nail 1. They are an important form of microbial growth occurring as complex cell populations primarily constructed of yeast-form and hyphal cells (e.g. **Figure 16(b)**). Their formation is a sequential process which involves attachment to a subsurface, proliferation of the yeast cells over the surface and finally extrusion of hyphae (Fanning & Mitchell, 2012). We reason that the biofilms that invaded Ossuary 7 (the broken and repaired ossuary) and Nail 1 (**Figure 10**, **Figure 11**, **Figure 20**) may have been in an amiable, perhaps symbiotic relationship with the neighbouring fungi, if so presenting us with an amazing example of a bacterial-fungal interaction (BFI). Bastias (et al., 2019) for example, have shown that many bacteria generate such a symbiotic relationship with plant-eating fungi. In this respect, we question the possibility that the biofilms acted as a kind of *umbilical cord* between the Ss and Sg groups of spores (see encircled in **Figure 20(a)**, right of center).

Based on our collective data above involving the full range of fungal infestation phenomena we reason that the fungal species that colonized the Cft are of the Yeast Kingdom of which at least 1500 species have been recognized. Similar to our unusual range of spore sizes and unlike in most fungal species, yeast spore sizes are known to vary greatly even within a single species, with the 3 - 4  $\mu\text{m}$  diameter (our Ss spores?) most common (e.g. Lema et al., 2012). Many yeast species (e.g. *Saccharomyces cerevisiae*) convert carbohydrates to carbon dioxide and alcohol during the fermentation process and the products of this process have been used in baking and production of alcohol for thousands of years, the fungi in the Caiaphas tomb may be testimony to just that. Although our fungi lack the “budding” morphology of *Saccharomyces*, we reason they may be a close variant of this species. A potential source of yeast fungi in the Caiaphas tomb could have been the family of the high priest Caiaphas (1<sup>st</sup> century CE)

whose home with its kitchens and wine cellar must have been near the family tomb. A possible alternative, or additional source of the yeast fungus could have been, some 1900 years later, the British headquarters during the Mandate period in early 20<sup>th</sup> century Palestine. This imposing and still existing structure on the Hill of Evil Council was constructed next to the ancient aqueduct (**Figure 1**), almost certainly an important source of water to Government House. We suggest that the yeast fungus may have been widely used not only in the Caiaphas family household but also ~1900 years later in the British Government House kitchens for the production of baked goods and alcohol. If so, the aqueduct whose ~60 km route from near Bethlehem to Jerusalem's Temple Mount may have been an important source of not only water for the Temple but also the carrier of what appears to be a very special fungal species into the tomb of the Caiaphas family. We had communicated with a number of scientists in the field of fungal biology regarding the complex fungal species here discussed and would like to quote from a recent mail exchange with R. Blanchette, Professor of Plant Pathology at the University of Minnesota. We quote "*You have put together some very interesting information. These observations are very different from the type of decay and fungi that we have found in various tombs and dry environments. It is amazing you are able to get this information from just a few minute segments of wood and bone adhering to the nails*".

## 9. Conclusion

In spite of the little material available to us for study, we have been able to determine that the long chain of sedimentary, geochemical and microbial events which affected the interior of the Caiaphas tomb ossuaries and the two nails were identical through a major part of their ~1900 year history (**Table 3**). The various components of fungi although much phosphatized, or petrified by iron oxides, have retained their original morphologies and are thus recognizable amongst the degraded bone debris but also on the wood fragments accreted to the nails. We cannot comment on the possible significance, if any, of the wood accreted on the nails being cedar (*Cedrus Libani*). Cedar did not grow in Early Iron age Palestine where it was a rare and expensive import which, according to the Old Testament, was used in construction of the Temple in Jerusalem (circa 970 to 931 BCE). Since cedar rejects wood rot some of its timber was also used in the construction of what is referred to as the "Jesus Boat". Although this, now excavated, small fishing vessel sank in the Sea of Galilee in the 1<sup>st</sup> century CE no implications have been made that it had any historical connection with Jesus of Nazareth. Reuven (2013) attempted to show that some wooden beams of cedar may have been used in construction on the Herodian period (1<sup>st</sup> century CE) Temple Mount in Jerusalem—the period of Caiaphas' rule.

Due to the lack of any evidence to support the hypothesis, we contest the proposal that the nails found in the Caiaphas tomb (Greenhut, 2004; Rahmani, 1961) were used for carving the decorative motives or were used for inscribing

the names on the ossuaries. Besides the problematic morphology of the nails we also take into consideration that inside one of the skulls in the tomb a coin was found, this may perhaps be attributed to a known pagan practice whereby the coin was meant as a payment to Charon—the ferryman of the Underworld. Thus far only one other nail has ever been found inside an ossuary (the Yehohanan Heel Bone nail, **Figure 8** above, [Tsaferis, 1985](#)) and that nail has been the only recorded archaeological artifact specifically identified with crucifixion. The presence in a burial context of what appear to be two crucifixion nails in the tomb of Caiaphas may, as the coin above, be more than a simple curiosity, rather they may be related to the fact that both Jewish and other sources identify nails used in a crucifixion as amulets possessing magical properties (ref. above). It follows that the presence of two nails with slivers of accreted cedar wood containing trace remains of bone tissue, present in two different ossuaries in the tomb of Caiaphas, suggests that, although neglected, these rare artifacts were an important issue in the family of the high priest. In consequence of the full range of observations above we feel confident in concluding that 1) the nails that we sampled are the missing nails from the Caiaphas family tomb and 2) these nails were, very probably, used in a crucifixion.

### Acknowledgements

We thank Dr. S. Freeman of the Volcani Institute of Agricultural Research, and Dr. R. Engesser of the Swiss Federal Institute for Forest, Snow and Landscape Research who helped in our efforts at identifying some of the fungal and bacterial morphologies. Professor R. A. Blanchette University of Minnesota examined some of the SEM micrographs and was able to provide tremendous assistance especially regarding the possible fungal species we have dealt with above. Dr. V. Uvarov assisted in the processing of some of the XRD analyses on nail samples carried out at the Center for Nanoscience and Nanotechnology at the Hebrew University. Special thanks go to Prof. A.R. Philpotts, University of Connecticut (ret.) for his constructive comments made to an earlier version of the present manuscript. Professor K. T. Kilty read and improved the manuscript's present format. Professor I. Herskovitz of the Medical Faculty Dept. of Anthropology Tel Aviv University introduced us to the nails, and in spite of the destructive process involved, very kindly permitted us to scrape off small amounts of material from both nails for study. Professor A. Frumkin, Dept. of Earth and Planetary Sciences, Hebrew University, and Dr. A. Ayalon of the Geological Survey of Israel made minor corrections in the  $\delta^{18}\text{O}$  and  $\delta^{13}\text{C}$  data table and offered suggestions regarding the interpretation of the values. Very special thanks go to Professor J. D. Tabor, previously chair of Religious Studies at the University of North Carolina, Charlotte and journalist and researcher S. Jacobovici, without their ideas and vision regarding certain contested archaeological finds linked to early Christianity in Jerusalem this project would be a non-starter. To you all and others we may have unintentionally neglected to mention, our deep gratitude.

## Conflicts of Interest

The authors declare no conflicts of interest regarding the publication of this paper.

## References

- Bar-Matthews, M., & Ayalon, A. (2001). *Carbonate Cave Deposits (Speleothems) as Palaeoclimate, Paleohydrological and Paleoseismic Indicators*. Report GSI/41/01.
- Bar-Matthews, M., & Ayalon, A. (2004). Speleothems as Palaeoclimate Indicators, a Case Study from Soreq Cave Located in the Eastern Mediterranean Region, Israel. In R. W. Battarbee, F. Gasse, & C. E. Stickley (Eds.), *Past Climate Variability through Europe and Africa* (pp. 363-391). Dordrecht: Springer.  
[https://doi.org/10.1007/978-1-4020-2121-3\\_18](https://doi.org/10.1007/978-1-4020-2121-3_18)
- Bastias, D. A., Johnson, L. J., & Card, S. D. (2019). Symbiotic Bacteria of Plant-Associated Fungi: Friends or Foes? *Current Opinion in Plant Biology*, *56*, 1-8.  
<https://doi.org/10.1016/j.pbi.2019.10.010>
- Blanchette, R. A., & Simpson, E. (1992). Soft Rot and Wood Pseudomorphs in an Ancient Coffin (700 BC) from Tumulus MM at Gordion, Turkey. *IAWA Bulletin n.s.*, *13*, 204-213. <https://doi.org/10.1163/22941932-90001269>
- Casanova, P. L., Haderlain, S. B., & Kappler, A. (2010). Biomineralization of Lepidocrocite and Goethite by Nitrate-Reducing Fe(II)-Oxidizing Bacteria: Effect of pH, Bicarbonate, Phosphate, and Humic Acids. *Geochimica et Cosmochimica Acta*, *74*, 3721-3734.  
<https://doi.org/10.1016/j.gca.2010.03.037>
- Cumplido, J., Barron, V., & Torrent, J. (2000). Effect of Phosphate on the Formation of Nanophase Lepidocrocite from Fe (II) Sulfate. *Clays and Clay Minerals*, *48*, 503-510.  
<https://doi.org/10.1346/CCMN.2000.0480502>
- Fanning, S., & Mitchell, A. P. (2012). Fungal Biofilms. *PLOS Pathogens*, *8*, e1002585.  
<https://doi.org/10.1371/journal.ppat.1002585>
- Frumkin, A., Ford, D. C., & Schwarcz, H. P. (1999). Continental Oxygen Isotopic Record of the Last 170,000 Years in Jerusalem. *Quaternary Research*, *51*, 317-327.  
<https://doi.org/10.1006/qres.1998.2031>
- Greenhut, Z. (1992). Burial Cave of the Caiaphas Family. *Biblical Archaeological Review*, *18*, 29-36.
- Greenhut, Z. (2004). *Discovery of the Caiaphas Family Tomb*. Jerusalem Perspective Online, Jan. 1. <http://www.jerusalemerspective.com>
- Hachlili, R., & Killebrew, A. (1983). Was the Coin-on-Eye Custom a Jewish Burial Practice in the Second Temple Period? *BA* 147-153. <https://doi.org/10.2307/3209825>
- Jacobovici, S. (2014). *Biblical Conspiracies Series, Nails of the Cross, 2014*.
- Kirschvink, J. L., Kobayashi-Kirschvink, A., & Woodford, B. J. (1992). Magnetite Biomineralization in the Human Brain. *Proceedings in the National Academy of Sciences* (Vol. 89, pp. 7683-7687). <https://doi.org/10.1073/pnas.89.16.7683>
- Lema, K. A., Willis, B. L., & Bourne, D. G. (2012). Corals Form Characteristic Associations with Symbiotic Nitrogen-Fixing Bacteria. *Applied and Environmental Microbiology*, *78*, 3136-3144. <https://doi.org/10.1128/AEM.07800-11>
- Lowenstam, H. A. (1981). Minerals Formed by Organisms. *Science*, *211*, 1126-1131.  
<https://doi.org/10.1126/science.7008198>
- Reuven, P. (2013). Wooden Beams from Herod's Temple Mount: Do They Still Exist? *Biblical Archaeology Review*, *39*, 40-47.

- Rahmani, L. (1961). Jewish Rock-Cut Tombs in Jerusalem. *Atiqot*, 3, 93-120.
- Ross, J. G., & Wang, C. (1982). Lepidocrocite in a Calcareous, Well-Drained Soil. *Clays and Clay Minerals*, 30, 394-396. <https://doi.org/10.1346/CCMN.1982.0300511>
- Schieber, J., & Glamoclija, M. (2007). Microbial Mats Built by Iron Bacteria: A Modern Example from Southern Indiana. In J. Schieber et al. (Eds.), *Atlas of Microbial Mat Features Preserved within the Clastic Rock Record* (pp. 233-244). Amsterdam: Elsevier.
- Shimron, A. E., Shirav, M., Kilty, K. T., Halicz, L., Pedersen, R. B., & Furnes, H. (2020). The Geochemistry of Intrusive Sediment Sampled from the 1st Century CE Inscribed Ossuaries of James and the Talpiot Tomb, Jerusalem. *Archaeological Discovery*, 8, 92-115.
- Schwertmann, U., & Taylor, R. M. (1972). The Transformation of Lepidocrocite to Goethite. *Clays and Clay Minerals*, 20, 151-158. <https://doi.org/10.1346/CCMN.1972.0200306>
- Tabor, J. D., & Jacobovici, S. (2012). *The Jesus Discovery*. New York: Simon and Schuster.
- Toynbee, J. M. C. (1971). *Death and Burial in the Roman World*. London: Johns Hopkins University Press.
- Trueman, C. et al. (2004). Mineralogical and Compositional Changes in Bones Exposed on Soil Surfaces in Amboseli National Park, Kenya: Diagenetic Mechanisms and the Role of Sediment Pore Fluids. *Journal of Archaeological Science*, 31, 721-739. <https://doi.org/10.1016/j.jas.2003.11.003>
- Tsaferis, V. (1985). Crucifixion—The Archaeological Evidence. *Biblical Archaeological Review*, 11, 44-53.
- Vaks, A. et al. (2003). Paleoclimate Reconstruction Based on the Timing of Speleothem Growth and Oxygen and Carbon Isotope Composition in a Cave Located in the Rain Shadow in Israel. *Quaternary Research*, 59, 182-193. [https://doi.org/10.1016/S0033-5894\(03\)00013-9](https://doi.org/10.1016/S0033-5894(03)00013-9)